

Sandro Mereghetti · Paolo Esposito · Andrea Tiengo

XMM–Newton observations of Soft Gamma-ray Repeaters

Presented at the conference "Isolated Neutron Stars: from the Surface to the Interior", London, UK, 24–28 April 2006

Abstract All the confirmed Soft Gamma-ray Repeaters have been observed with the EPIC instrument on the XMM–Newton satellite. We review the results obtained in these observations, providing the most accurate spectra on the persistent X-ray emission in the 1–10 keV range for these objects, and discuss them in the context of the magnetar interpretation.

Keywords gamma-rays: observations · pulsars: individual SGR 1806–20, SGR 1900+14, SGR 1627–41 · pulsars: general

PACS 97.60.Jd · 98.70.Qy

1 Introduction

Soft Gamma-ray Repeaters (SGRs) were discovered as sources of short intense bursts of gamma-rays, and for a long time were considered as a puzzling category of Gamma-ray bursts. Their neutron star nature was immediately suggested by the 8 s periodicity seen in the famous event of 5 March 1979, but it was only with the discovery of their pulsating counterparts in the few keV region that this was finally proved. Although the main motivations for the magnetar model (Duncan & Thompson 1992; Thompson & Duncan 1995) were driven by the high energy properties of the SGRs bursts and giant flares, X-ray observations of the “quiescent” emission have provided fundamental information to understand the nature of these objects (Woods & Thompson 2004).

Extensive observational programs have been carried out with the RossiXTE satellite, focusing mainly on the SGRs timing properties. Long term studies based on phase-connected timing analysis revealed significant deviations from a steady spin-down (Woods et al. 1999a, 2000, 2002),

S. Mereghetti, A. Tiengo
INAF – Istituto di Astrofisica Spaziale e Fisica Cosmica, Milano, Italy

P. Esposito
Università di Pavia, Dipartimento di Fisica Nucleare e Teorica and INFN-Pavia, Italy

larger than the timing noise seen in radio pulsars and not linked in a simple way with the bursting activity. RossiXTE has also been used to investigate the variations of the pulse profiles as a function of energy and time (Göğüş et al. 2002), and to study the statistical properties of the bursts (Göğüş et al. 2001). However, the RossiXTE observations are not ideal to accurately measure the flux and spectrum of these relatively faint sources located in crowded fields of the Galactic plane, since its non-imaging instruments suffer from source confusion and large uncertainties in the background estimate. Imaging satellites like BeppoSAX, ASCA and Chandra have yielded useful spectral information, but it is only with the advent of the large collecting area XMM–Newton satellite that high quality spectra of SGRs have been obtained, in particular with the EPIC instrument (Strüder et al. 2001; Turner et al. 2001).

Here we review the results obtained with the XMM–Newton satellite for the three confirmed SGRs in our Galaxy. There are also some XMM–Newton data on SGR 0526–66 in the Large Magellanic Cloud, but they are of limited use due to the contamination from diffuse emission from the surrounding supernova remnant and will not be discussed here.

2 SGR 1806–20

SGR 1806–20 is probably the most prolific and the best studied of the known SGRs. It showed several periods of bursting activity since the time of its discovery in 1979 (Laros et al. 1986) and recently attracted much interest since it emitted the most powerful giant flare ever observed from an SGR (Hurley et al. 2005; Palmer et al. 2005; Mereghetti et al. 2005a).

The low energy X-ray counterpart of SGR 1806–20 was identified with the ASCA satellite (Murakami et al. 1994), thanks to the detection and precise localization of a burst simultaneously seen at higher energy with BATSE. Subsequent observations with RossiXTE led to the discovery of pulsations with $P=7.5$ s and $\dot{P}=8\times 10^{-11}$ s s⁻¹ (Kouveliotou et al. 1998).

Table 1 XMM–Newton observations and timing results for SGR 1806–20.

Obs.	Date	Duration (ks)	Mode ^(a) and exp. time PN camera	Mode ^(a) and exp. time MOS1/2 cameras	Pulse Period (s)
A	2003 Apr 3	32	FF (5.4 ks)	LW (6 ks)	7.5311±0.0003
B	2003 Oct 7	21	FF (13.4 ks)	LW (17 ks)	7.5400±0.0003
C	2004 Sep 6	51	SW (36.0 ks)	LW (51 ks)	7.55592±0.00005
D	2004 Oct 6	18	SW (12.9 ks)	Ti (18 ks)	7.5570±0.0003
E	2005 Mar 7	24	SW (14.7 ks)	Ti/FF (24 ks)	7.5604±0.0008
F	2005 Oct 4	33	SW (22.8 ks)	Ti/FF (33 ks)	7.56687±0.00003
G	2006 Apr 4	29	SW (20.5 ks)	Ti/FF (29 ks)	7.5809±0.0002

^(a) FF = Full Frame (time resolution 73 ms); LW = Large Window (time resolution 0.9 s); SW = Small Window (time resolution 6 ms); Ti = Timing (time resolution 1.5 ms)

Possible associations of SGR 1806–20 with the variable non-thermal core of a putative radio supernova remnant (Frail et al. 1997) and with a luminous blue variable star (van Kerkwijk et al. 1995) were disproved when a more precise localization of the SGR could be obtained with the Interplanetary Network (Hurley et al. 1999b) and later improved with Chandra (Kaplan et al. 2002). The transient radio source observed with the VLA after the December 2004 giant flare (Cameron et al. 2005) led to an even smaller error region and, thanks to the superb angular resolution (FWHM $\sim 0.1''$) available with adaptive optics at the ESO Very Large Telescope a variable near IR counterpart ($K_s=19.3-20$), could be identified (Israel et al. 2005), the first one for an SGR.

The distance of SGR 1806–20 is subject of some debate (Cameron et al. 2005), and is particularly relevant for its implications on the total energetics of the 2004 giant flare. A firm lower limit of 6 kpc can be derived from the HI absorption spectrum (McClure-Griffiths & Gaensler 2005), but the likely associations with a massive molecular cloud and with a cluster of massive stars indicate a distance of ~ 15 kpc (Corbel & Eikenberry 2004; Figer et al. 2005). In the following we will adopt this value.

Before the XMM–Newton observations, the most accurate spectral measurements for SGR 1806–20 in the soft X-ray range were obtained with BeppoSAX in 1998–1999 (Mereghetti et al. 2000). They showed that a power law with photon index $\Gamma=1.95$ or a thermal bremsstrahlung with temperature $kT_{tb}=11$ keV were equally acceptable fits. All the observations indicated a fairly constant flux, corresponding to a 2–10 keV luminosity of $\sim 3 \times 10^{35}$ erg s⁻¹.

Being located at only $\sim 10^\circ$ from the Galactic center direction, SGR 1806–20 has been extensively observed with the INTEGRAL satellite since 2003. A few hundreds bursts have been detected with the IBIS instrument in the 15–200 keV range, leading to the discovery of a hardness intensity anti-correlation and allowing to extend the number-flux relation of bursts down to fluences smaller than 10^{-8} erg cm⁻² (Götz et al. 2004, 2006b). In addition, it was discovered with INTEGRAL that the persistent emission from SGR 1806–20 extends up to 150 keV (Mereghetti et al. 2005b; Molkov et al. 2005). The hard X-ray emission, well fit by a power law with photon index $\Gamma \sim 1.5-1.9$, seems to correlate

in hardness and intensity with the rate of burst emission, that reached a maximum in Fall 2004.

The bursting activity of SGR 1806–20 culminated with the giant flare of 2004 December 27 (Borkowski et al. 2004; Hurley et al. 2005; Palmer et al. 2005), that produced the strongest flash of gamma-rays at the Earth ever observed. The emission was so intense to cause saturation of most in-flight detectors, significant ionization of the upper atmosphere (Campbell et al. 2005), and a detectable flux of radiation backscattered from the Moon (Mazets et al. 2005; Mereghetti et al. 2005a). Other observations of this exceptional event, and their implications for the physics of neutron stars, are discussed elsewhere in these proceedings (Stella 2006; Israel 2006). Comparing this giant flare with those seen from SGR 0526–66 and SGR 1900+14, it is found that the energy in the pulsating tails of the three events was roughly of the same order ($\sim 10^{44}$ ergs), while the energy in the initial spike of SGR 1806–20 (a few 10^{46} ergs) was at least two orders of magnitude higher than that of the other giant flares. This indicates that the magnetic field in the three sources is similar. In fact the pulsating tail emission is thought to originate from the fraction of the energy released during the initial hard pulse that remains magnetically trapped in the neutron star magnetosphere, forming an optically thick photon-pair plasma (Thompson & Duncan 1995). The amount of energy that can be confined in this way is determined by the magnetic field strength, which is thus inferred to be of several 10^{14} G in these three magnetars.

SGR 1806–20 is the target of an ongoing campaign of XMM–Newton observations aimed at studying in detail the long term variations in the properties of its persistent emission. These observations, coupled with similar programs carried out with ESO telescopes in the infrared band (Israel 2006) and at hard X-ray energy with INTEGRAL (Götz et al. 2006a) and Suzaku, can be used to study the connection between the persistent emission and the source activity level, as manifested by the emission of bursts and flares.

2.1 XMM–Newton results

Seven XMM–Newton observations of SGR 1806–20 have been carried out to date (see Table 1). Four were obtained from April 2003 to October 2004, before the giant flare

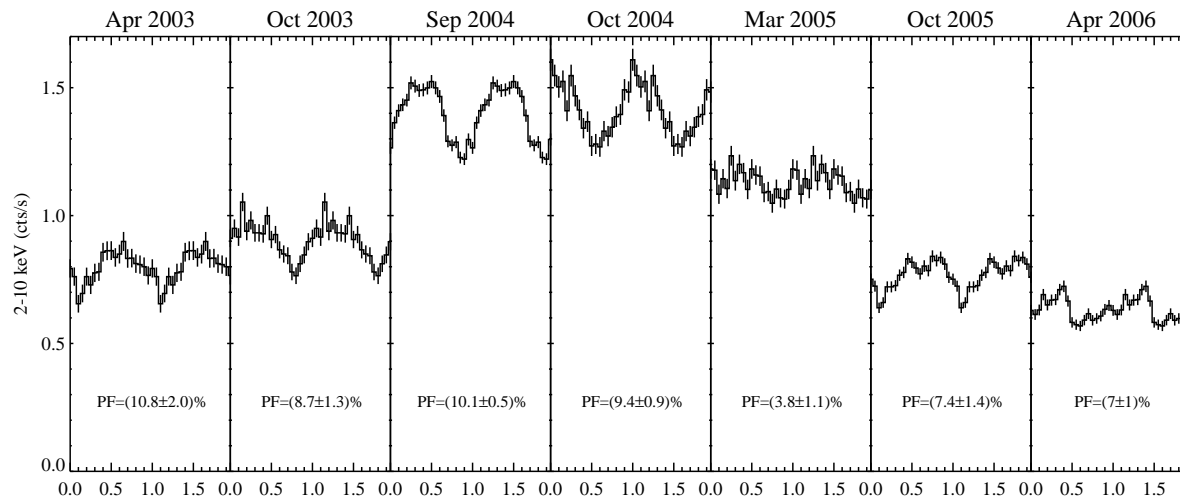


Fig. 1 Folded light curves of SGR 1806–20 obtained with the EPIC pn instrument in the seven XMM–Newton observations. Note the flux increase in the two observations before the December 2004 giant flare and the small pulsed fraction in the first 2005 observation.

Table 2 Summary of the spectral results^(a) for SGR 1806–20

Obs.	Absorption 10^{22} cm^{-2}	Power Law photon index	kT_{BB} (keV)	R_{BB} (km) ^(b)	Flux ^(c) $10^{-11} \text{ erg cm}^{-2} \text{ s}^{-1}$	χ^2_{red} (d.o.f.)
A	6.6 (5.6–8.4)	1.4 (1.0–1.7)	0.6 (0.4–0.9)	2.6 (0.7–13.9)	1.23	1.01 (56)
B	6.0 (4.9–6.6)	1.2 (0.5–1.4)	0.7 (0.6–1.0)	1.8 (1.2–2.9)	1.39	0.97 (68)
C	6.5 (6.2–6.9)	1.21 (1.09–1.35)	0.8 (0.7–0.9)	1.9 (1.6–2.6)	2.66	0.93 (70)
D	6.5 (5.9–7.1)	1.2 (0.9–1.4)	0.8 (0.6–0.9)	2.2 (1.6–3.5)	2.68	0.90 (69)
E	6.0 (5.8–6.2)	0.8 (0.5–1.0)	0.91 (0.86–1.05)	1.9 (1.6–2.1)	1.92	1.02 (70)
F	6.4 (6.0–6.8)	1.4 (1.1–1.7)	0.7 (0.6–0.8)	2.2 (1.7–3.3)	1.34	1.11 (69)
G	6.2 (5.6–6.6)	1.2 (0.9–1.4)	0.7 (0.6–0.8)	2.0 (1.6–2.7)	1.07	1.09 (68)

^(a) Errors are at the 90% c.l. for a single interesting parameter

^(b) Radius at infinity assuming a distance of 15 kpc

^(c) Absorbed flux in the 2–10 keV energy range

(Mereghetti et al. 2005c). At the time of the giant flare the source was not visible by XMM–Newton (and most other satellites) due to its proximity to the Sun, thus the next observation could be done only in March 2005 (Tiengo et al. 2005). This was followed by another observation in October (Rea et al. 2005) and a most recent one in April 2006, the results of which are presented here for the first time.

The bursts detected in some of these observations (mostly in September–October 2004) were excluded by appropriate time selections to derive the spectral results reported below. After screening out the bursts, the source pulsations were clearly detected in all the observations. The corresponding folded light curves are shown in Fig. 1, where all the panels have the same scale in count rate to facilitate a comparison of the flux variations between the observations. The main spectral results are summarized in Table 2, where we have reported only the best fit parameters for the power law plus blackbody model (see Mereghetti et al. 2005c; Tiengo et al. 2005 for more details).

Indeed the strong requirement for a blackbody component is one of the main results of the high quality XMM–Newton spectra. In this respect the most compelling evi-

dence comes from the September 2004 observation (obs. C), which, thanks to the high source count rate and long observing time, provided the spectra with the best statistics. A fit with an absorbed power law yields a relatively high χ^2 value ($\chi^2_{red}=1.37$) and structured residuals, while a much better fit ($\chi^2_{red}=0.93$) can be obtained by adding a blackbody component. The best fit parameters are photon index $\Gamma=1.2$, blackbody temperature $kT_{BB}=0.8$ keV and absorption $N_H \sim 6.5 \times 10^{22} \text{ cm}^{-2}$. Although some of the observations with lower statistics give acceptable fits also with a single power law, the results reported in Table 2 indicate that all the observations are consistent with the presence of an additional blackbody component with similar parameters.

The second new result derived from these observations is the long term flux variability. All the observations of SGR 1806–20 in the 1–10 keV range obtained in the previous years with ROSAT, ASCA and BeppoSAX were consistent with a flux of $\sim 10^{-11} \text{ erg cm}^{-2} \text{ s}^{-1}$. On the other hand, the XMM–Newton data showed a doubling of the flux in September–October 2004 followed by a gradual recovery to the “historical” level during the observations performed after the gi-

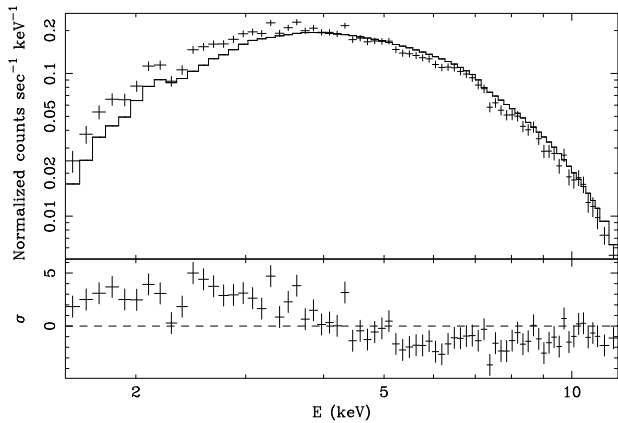


Fig. 2 Top panel: the data represent the spectrum of obs. G, while the line is the best fit model of obs. C simply rescaled in normalization. The residuals shown in the bottom panel clearly indicate that the spectrum was softer after the giant flare.

ant flare. Interestingly, the same trend was seen above 20 keV with INTEGRAL (Mereghetti et al. 2005b; Götz et al. 2006a), as well as in the flux of the NIR counterpart (Israel et al. 2005; Israel 2006).

The observations performed before and after the giant flare show significant differences also in the source pulsed fraction and spectral shape. The pulsed fraction in the first observation after the flare was the smallest seen with XMM–Newton, while it increased again in the following observations. The spectral hardness followed a similar trend: the four pre-flare observations give marginal evidence for a gradual hardening, while the spectrum was definitely softer in the post-flare observations. This is illustrated in Fig. 2, which shows the April 2006 spectrum fitted with the pre-flare model (obs. C): the trend in the residuals clearly indicate the spectral softening.

Finally, we can compare the XMM–Newton spectra with those obtained in the previous years with other satellites. We base this comparison on the fits with a single power law, since this model was successfully used to describe the ASCA and BeppoSAX data. The average photon index in the four XMM–Newton observations of 2003–2004 ($\Gamma=1.5 \pm 0.1$) was significantly smaller than that observed in 1993 with ASCA ($\Gamma=2.25 \pm 0.15$, Mereghetti et al. 2002) and in 1998–2001 with BeppoSAX ($\Gamma=1.97 \pm 0.09$, Mereghetti et al. 2002). This indicates that a spectral hardening occurred between September 2001 and April 2003.

A long term variation occurred also in the average spin-down rate: while the early sparse period measurements with ASCA and BeppoSAX (Mereghetti et al. 2002), as well as a phase-connected RossiXTE timing solution spanning February–August 1999 (Woods et al. 2000), were consistent with an average $\dot{P} \sim 8.5 \times 10^{-11} \text{ s s}^{-1}$, subsequent RossiXTE data indicate a spin-down larger by a factor ~ 4 (Woods et al. 2002) and the four XMM–Newton period measurements before the giant flare show a further increase to an average $\dot{P}=5.5 \times 10^{-10} \text{ s s}^{-1}$ (Mereghetti et al. 2005c).

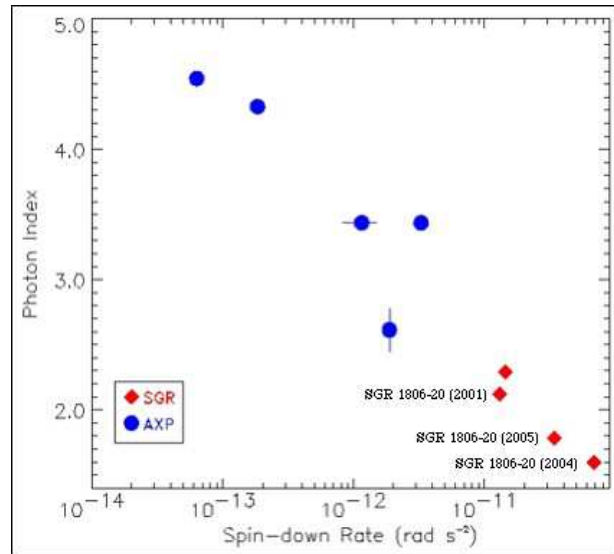


Fig. 3 Correlation between power law photon index and spin-down rate in Anomalous X-ray Pulsars and SGRs (adapted from Marsden & White 2001). Each point refers to a different source, except the three points for SGR 1806–20 in different time periods.

As shown in Fig. 3, the changes in spectral hardness and spin-down rate of SGR 1806–20 follow the correlation between these quantities discovered in the sample of AXPs and SGRs by comparing different objects: the sources with the harder spectrum have a larger long term spin-down rate (Marsden & White 2001). These results indicate, for the first time, that such a correlation also holds within different states of a single source.

3 SGR 1900+14

Bursts from this SGR were discovered with the Venera satellites in 1979 (Mazets et al. 1979). No other bursts were detected until thirteen years later, when four more events were seen with BATSE in 1992 (Kouveliotou et al. 1993). In the meantime the X-ray counterpart had been discovered with ROSAT (Vasisht et al. 1994), and later found to pulsate at 5.2 s with ASCA (Hurley et al. 1999c). Subsequent observations with the RossiXTE satellite confirmed the pulsations and established that the source was spinning down rapidly, with a period derivative of $\sim 10^{-11} \text{ s s}^{-1}$ (Kouveliotou et al. 1999).

The peak of the activity from SGR 1900+14 was reached on 1998 August 27, with the emission of a giant flare (Hurley et al. 1999a; Feroci et al. 1999), resembling the only similar event known at that time, the exceptional burst of 5 March 1979. The 1998 giant flare from SGR 1900+14 could be studied much better than that of SGR 0526–66. The flare started with a short ($\sim 0.07 \text{ s}$) soft spike, followed by a much brighter short and hard pulse that reached a peak luminosity of $\sim 10^{45} \text{ erg s}^{-1}$. The initial spike was followed by a softer gamma-ray tail modulated at 5.2 s (Hurley et al. 1999a; Mazets et al.

1999), which decayed in a quasi exponential manner over the next ~ 6 minutes (Feroci et al. 2001). Integrating over the entire flare assuming isotropic emission, at least 10^{44} erg were released in hard X-rays above 15 keV (Mazets et al. 1999). SGR 1900+14 also emitted another less intense flare on 18 April 2001 (Feroci et al. 2003; Guidorzi et al. 2004), which based on its energetics was classified as an “intermediate” flare.

Despite being the less absorbed of the galactic SGRs ($N_H \sim 2 \times 10^{22} \text{ cm}^{-2}$) no optical/IR counterpart has been yet identified for SGR 1900+14. Its possible association with a young cluster of massive stars (Vrba et al. 2000), where the SGR could have been born, gives a distance of ~ 15 kpc, that we will adopt in the following.

Recently, persistent emission from SGR 1900+14 has been detected also in the 20–100 keV range thanks to observations with the INTEGRAL satellite (Götz et al. 2006b).

3.1 XMM–Newton results

SGR 1900+14 lies in a sky region that, until recently, was not observable by XMM–Newton due to technical constraints in the satellite pointing. Thus the first observation of SGR 1900+14 could be obtained only in September 2005 (Mereghetti et al. 2006b). This observation occurred during a long period of inactivity (the last bursts before the observations were reported in November 2002, Hurley et al. 2002).

The spectrum could not be fit satisfactorily with single component models, while a good fit was obtained with the sum of a power law and a blackbody, with photon index $\Gamma=1.9\pm 0.1$, temperature $kT=0.47\pm 0.02$ keV, absorption $N_H = (2.12 \pm 0.08) \times 10^{22} \text{ cm}^{-2}$, and unabsorbed flux $\sim 4.8 \times 10^{-12} \text{ erg cm}^{-2} \text{ s}^{-1}$ (2–10 keV). An acceptable fit could also be obtained with the sum of two blackbodies with temperatures of 0.53 and 1.9 keV.

The XMM–Newton power law plus blackbody parameters are in agreement with previous observations of this source carried out with ASCA (Hurley et al. 1999c), BeppoSAX (Woods et al. 1999b; Esposito et al. 2006) and Chandra (Kouveliotou et al. 2001), but the flux measured in September 2005 is the lowest ever seen from SGR 1900+14. A $\sim 30\%$ decrease of the persistent emission, compared to the “historical” level of $\sim 10^{-11} \text{ erg cm}^{-2} \text{ s}^{-1}$, had already been noticed in the last BeppoSAX observation (Esposito et al. 2006), that was carried out in April 2002, six month earlier than the last bursts reported before the recent reactivation. The long term fading experienced by SGR 1900+14 in 2002–2005 might be related to the apparent decrease in the bursting activity in this period.

A second XMM–Newton observation was carried out on 1 April 2006, as a target of opportunity following the source reactivation indicated by a few bursts detected by Swift (Palmer et al. 2006) and Konus-Wind (Golenetskii et al. 2006). The spectral shape was consistent with that measured in the first observation, but the flux was $\sim 5.5 \times 10^{-12} \text{ erg cm}^{-2} \text{ s}^{-1}$ (Mereghetti et al. 2006b).

The spin period was 5.198346 ± 0.000003 s in September 2005 and 5.19987 ± 0.00007 s in April 2006. In both observations the pulsed fraction was $\sim 16\%$ and no significant changes in the pulse profile shape were seen after the burst reactivation.

For both observations we performed phase-resolved spectroscopy extracting the spectra for different selections of phase intervals. No significant variations with phase were detected, all the spectra being consistent with the model and parameters of the phase-averaged spectrum, simply rescaled in normalization.

4 SGR 1627–41

From the point of view of the bursts and timing properties, SGR 1627–41 is one of the less well studied SGRs. This source was discovered during a period of bursting activity that lasted only six weeks in 1998 (Woods et al. 1999c; Hurley et al. 1999d; Mazets et al. 1999). Since then no other bursts were observed.

With a column density of $N_H \sim 10^{23} \text{ cm}^{-2}$, corresponding to $A_V \sim 40\text{--}50$, SGR 1627–41 is the most absorbed of the known SGRs. Thus it is not surprising that little is known on its possible counterparts. Near IR observations (Wachter et al. 2004) revealed a few objects positionally consistent with the small Chandra error region, but they are likely foreground objects unrelated to the SGR.

A distance of 11 kpc is generally assumed for SGR 1627–41, based on its possible association with the radio complex CTB 33, comprising the supernova remnant SNR G337.0–0.1 and a few HII regions (Corbel et al. 1999).

During the active period a soft X-ray counterpart with flux $F_x \sim 7 \times 10^{-12} \text{ erg cm}^{-2} \text{ s}^{-1}$ was identified with BeppoSAX (Woods et al. 1999c). However it was not possible to reliably measure a periodicity (a marginal detection at 6.4 s was not confirmed by better data).

Observations carried out in the following years with BeppoSAX, ASCA and Chandra showed a monotonic decrease in the luminosity, from the value of $\sim 10^{35} \text{ erg s}^{-1}$ (for $d=11$ kpc) seen in 1998 down to $\sim 4 \times 10^{33} \text{ erg s}^{-1}$.

4.1 XMM–Newton results

A 52 ks long XMM–Newton pointing on SGR 1627–41 was done in September 2004 (Mereghetti et al. 2006a), while some other information could be extracted from two observations in which SGR 1627–41 was serendipitously detected at an off-axis angle of $\sim 10'$. These ~ 30 ks long observations, whose main target was IGR J16358–4726, were carried out in February and September 2004.

All the XMM–Newton data showed a rather faint source ($\sim 9 \times 10^{-14} \text{ erg cm}^{-2} \text{ s}^{-1}$) with a soft spectrum. Unfortunately the source faintness did not allow a sensitive search for periodicities. Both a steep power law (photon index $\Gamma = 3.7 \pm 0.5$) and a blackbody with temperature

Table 3 Main properties of the four confirmed SGRs

	SGR 1627–41	SGR 1806–20	SGR 1900+14	SGR 0526–66
Coordinates	16 ^h 35 ^m 51.83 ^s –47° 35′ 23.3″	18 ^h 08 ^m 39.337 ^s –20° 24′ 39.85″	19 ^h 07 ^m 14.33 ^s +09° 1′ 9 20.1″	05 ^h 26 ^m 00.89 ^s –66° 04′ 36.3″
Error	0.2″ [a]	0.06″ [b]	0.15″ [d]	0.6″ [g]
Distance	11 kpc	15 kpc	15 kpc	50 kpc
Period	–	7.6 s	5.2 s	8 s
Period derivative (s s ⁻¹)	–	(8.3 – 81) × 10 ⁻¹¹ [c]	(6.1 – 20) × 10 ⁻¹¹ [e]	6.6 × 10 ⁻¹¹ [g]
Magnetic field ^a	–	(8 – 25) × 10 ¹⁴ G	(6 – 10) × 10 ¹⁴ G	7 × 10 ¹⁴ G
Flux range ^b (erg cm ⁻² s ⁻¹)	(0.025 – 0.6) × 10 ⁻¹¹	(1.3 – 3.8) × 10 ⁻¹¹	(0.5 – 2.7) × 10 ⁻¹¹	0.07 × 10 ⁻¹¹
Typical flux ^b (erg cm ⁻² s ⁻¹)	~ 3 × 10 ⁻¹³	~ 1.5 × 10 ⁻¹¹	~ 10 ⁻¹¹	~ 10 ⁻¹²
20–60 keV flux (erg cm ⁻² s ⁻¹)	–	(3 – 5) × 10 ⁻¹¹	~ 1.5 × 10 ⁻¹¹	–
Optical/IR	J>21.5, H>19.5, K _s >20.0 [a]	K _s =20–19.3 [b] J>21.2, H>19.5	J>22.8, K _s >20.8 [f]	V>27.1, I>25 [h]
Luminosity ^c (erg s ⁻¹)	~ 4 × 10 ³³	~ 4 × 10 ³⁵	~ 3 × 10 ³⁵	~ 2 × 10 ³⁵
Photon index	3	1.2	2	3.1
Blackbody kT	–	0.8 keV	0.45 keV	0.53 keV
N _H	9 × 10 ²² cm ⁻²	6.5 × 10 ²² cm ⁻²	2.2 × 10 ²² cm ⁻²	0.55 × 10 ²² cm ⁻²
Giant Flare	–	December 27, 2004	August 27, 1998	March 5, 1979
Initial spike energy (erg)	–	(1.6 – 5) × 10 ⁴⁶	> 6.8 × 10 ⁴³	1.6 × 10 ⁴⁴
Pulsating tail energy (erg)	–	1.3 × 10 ⁴⁴	5.2 × 10 ⁴³	3.6 × 10 ⁴⁴
Most active periods	1998 Jun–Jul	1983–1985, 1996–1999, 2003–2004	1979 Mar, 1992, 1998–1999, 2001–2002, 2006	1979 Mar–Apr, 1981 Dec–1983 Apr

REFERENCES:

[a] (Wachter et al. 2004) [c] (Woods et al. 2006) [e] (Woods et al. 2002) [g] (Kulkarni et al. 2003)
[b] (Israel et al. 2005) [d] (Frail et al. 1999) [f] (Kaplan et al. 2002) [h] (Kaplan et al. 2001)

NOTES:

(^a) Assuming spin-down due to dipole radiation: $B = 3.2 \times 10^{19} (P\dot{P})^{1/2}$ G

(^b) Unabsorbed flux in the 2–10 keV energy range

(^c) Luminosity in the 2–10 keV energy range assuming the distances reported above

$kT_{BB} = 0.8^{+0.2}_{-0.1}$ keV gave acceptable fits. The absorption was consistent with that measured in all the previous observations, $N_H = 9 \times 10^{22}$ cm⁻². There is evidence that the spectrum softened between the two Chandra observations carried out in September 2001 and August 2002 (Kouveliotou et al. 2003). The photon index measured with XMM–Newton is consistent with that of the last Chandra observation but, due to the large uncertainties, also a further softening cannot be excluded.

The XMM–Newton flux measurements are compared with those obtained in previous observations in Fig. 4. The two panels refer to the observed (top) and emitted (bottom) fluxes in the 2–10 keV range and for a common value of the absorption in all the observations ($N_H = 9 \times 10^{22}$ cm⁻², see Mereghetti et al. 2006a for details). The long term decrease in luminosity is clear, but, owing to the source spectral variations, the details of the decay light curve are different for the observed and unabsorbed flux.

If one considers the observed fluxes, the Chandra and XMM–Newton data suggest that SGR 1627–41 continued to fade also after September 2001, while the unabsorbed values indicate a possible plateau level at $\sim 2.5 \times 10^{-13}$ erg cm⁻² s⁻¹. It is important to realize that the quantity most relevant for theoretical modeling, i.e. the emitted flux, is subject to the

uncertainties in the spectral parameters. This is particularly important for high N_H values and small fluxes, as in the case of SGR 1627–41.

The long term luminosity decrease of SGR 1627–41 was interpreted as evidence for cooling of the neutron star surface after the deep crustal heating that occurred during the period of SGR activity in 1998. The decay light curve was fitted with a model of deep crustal heating requiring a massive neutron star ($M > 1.5 M_\odot$) which could well explain a plateau seen between days 400 and 800 (Kouveliotou et al. 2003). However, the evidence for such a plateau is not so compelling, according to our reanalysis of the BeppoSAX data. In fact all the BeppoSAX and ASCA points in the top panel of Fig. 4, before the rapid decline seen with Chandra in September 2001, are well fit by a power law decay, $F(t) \propto (t - t_0)^{-0.6}$, where t_0 is the time of the discovery outburst.

5 XMM–Newton results on the SGRs bursts

Up to now limited spectral information has been obtained for SGR bursts below 20 keV. In particular, before our XMM–Newton observations, spectra with good energy resolution and sensitivity at a few keV were lacking. However, some

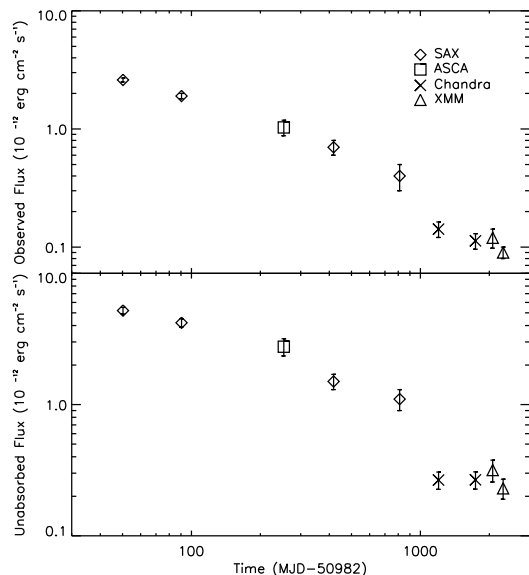


Fig. 4 Long term light curve of SGR 1627–41 based on data from different satellites (Mereghetti et al. 2006a). Top panel: absorbed flux in the 2–10 keV range. Bottom panel: unabsorbed flux in the 2–10 keV range. For clarity, the XMM–Newton points of 2004 September 4, which are consistent with the last measurement, are not plotted.

studies have provided evidence that the optically thin thermal bremsstrahlung model, which gives a good phenomenological description of the burst spectra in the hard X-ray range, is inconsistent with the data below 15 keV (Fenimore et al. 1994; Olive et al. 2004; Feroci et al. 2004). We therefore tried to address this issue using the XMM–Newton data.

Several tens of bursts were detected during some of the XMM–Newton observations of SGR 1806–20 (while none was seen in SGR 1900+14 and SGR 1627–41). These bursts had durations typical of the short bursts more commonly observed at higher energy. Since the individual bursts had too few counts for a meaningful spectral analysis, we extracted a cumulative spectrum by summing all the bursts detected during the 2004 observations. The resulting spectrum corresponds to a total exposure of 12.7 s and contains about 2000 net counts in the 2–10 keV range. We checked that pile-up effects were not important (see Mereghetti et al. 2005c for details). The spectrum of the remaining observing time was used as background.

All the fits with simple models (power law, blackbody, thermal bremsstrahlung) gave formally acceptable χ^2 values, but the power law and the bremsstrahlung required a large absorption ($N_H=10^{23}$ cm $^{-2}$), inconsistent with the value seen in the persistent emission. We therefore favor the blackbody model, which yields $kT_{BB}=2.3\pm 0.2$ keV and $N_H=6\times 10^{22}$ cm $^{-2}$, in agreement with the value determined from the spectrum of the persistent emission.

The residuals from this best fit showed a deviation at 4.2 keV. Although the deviation is formally at 3.3σ , it could not be reproduced in spectra obtained with different data selections and binning criteria. Therefore we consider it as

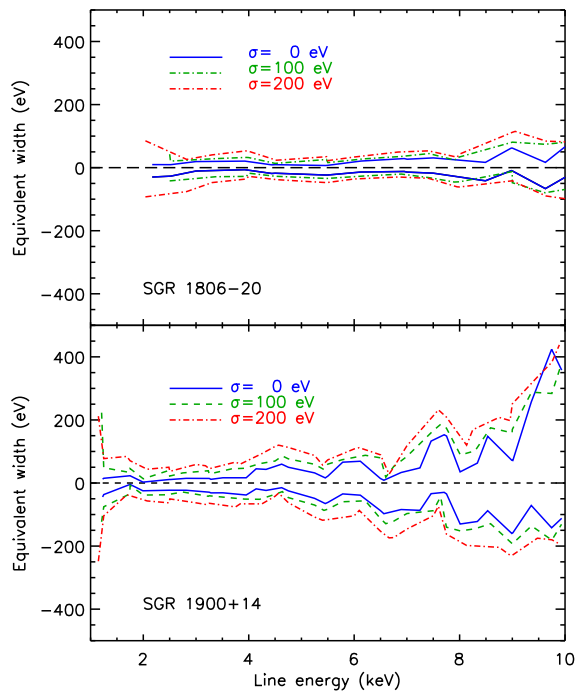


Fig. 5 Upper limits (at 3σ) on spectral features in the persistent emission of SGR 1806–20 (top) and SGR 1900+14 (bottom).

only a marginal evidence for an absorption line (Mereghetti et al. 2005c).

6 (Absence of) spectral lines

In models involving ultra-magnetized neutron stars, proton cyclotron features are expected to lie in the X-ray range, for surface magnetic fields strengths of $\sim 10^{14}$ – 10^{15} G. Detailed calculations of the spectrum emerging from the atmospheres of magnetars in quiescence have confirmed this basic expectation (Zane et al. 2001; Ho & Lai 2001). Model spectra exhibit a strong absorption line at the proton cyclotron resonance, $E_{c,p} \simeq 0.63z_G(B/10^{14}$ G) keV, where z_G , typically in the 0.70–0.85 range, is the gravitational red-shift at the neutron star surface. No evidence for persistent cyclotron features has been reported to date in SGRs, despite some features have been possibly detected during bursts (see e.g. Strohmayer & Ibrahim 2000; Ibrahim et al. 2003).

A sensitive search for spectral lines was among the main objectives of the XMM–Newton observations of SGRs. However no evidence for emission or absorption lines, was found by looking at the residuals from the best fit models. In the case of SGR 1806–20 and SGR 1900+14 the upper limits are the most constraining ever obtained for these sources in the ~ 1 –10 keV energy range. They are shown in Fig. 5 for the most sensitive observation of each source, i.e. those of September 2004 for SGR 1806–20 and of September 2005 for SGR 1900+14. The plotted curves represent the upper

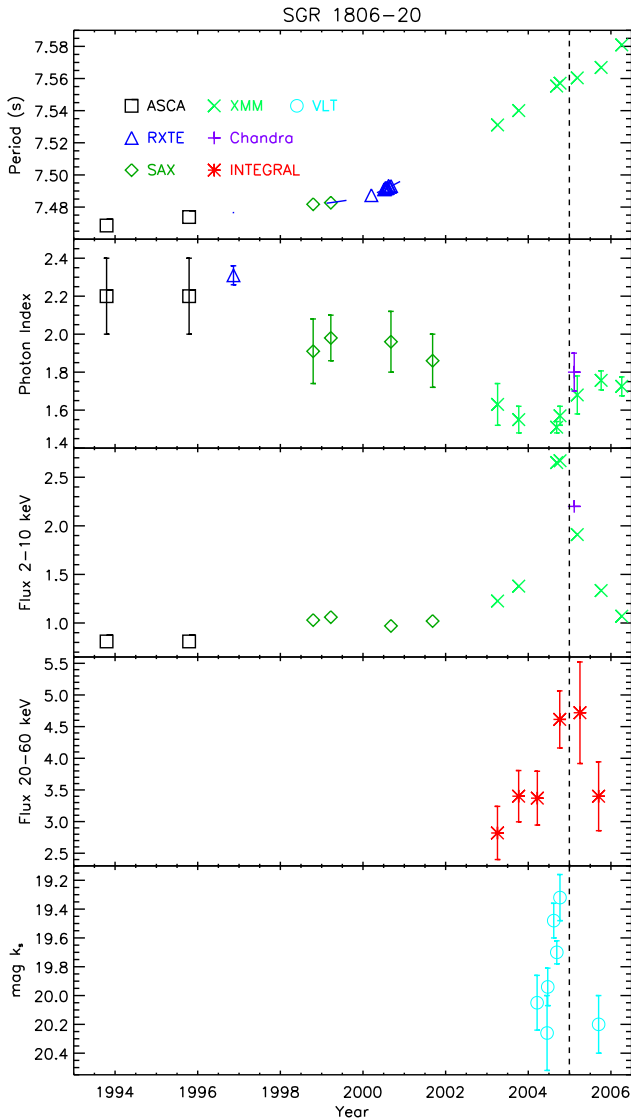


Fig. 6 From top to bottom: long term evolution of the pulse period, photon index, X-ray flux (2–10 keV), hard X-ray flux (20–60 keV), and infrared magnitude of SGR 1806–20. Fluxes are in units of 10^{-11} erg cm^{-2} s^{-1} . The vertical dashed line indicates the December 2004 giant flare.

limits on the equivalent widths as a function of the assumed line energy and width. They were derived by adding Gaussian components to the best fit models and computing the allowed range in their normalization.

Some reasons have been proposed to explain the absence of cyclotron lines in magnetars, besides the obvious possibility that they lie outside the sampled energy range. Magnetars might differ from ordinary radio pulsars because their magnetospheres are highly twisted and therefore can support current flows (Thompson et al. 2002). The presence of charged particles (e^- and ions) produces a large resonant scattering depth and since i) the electron distribution is spatially extended and ii) the resonant frequency depends on the local

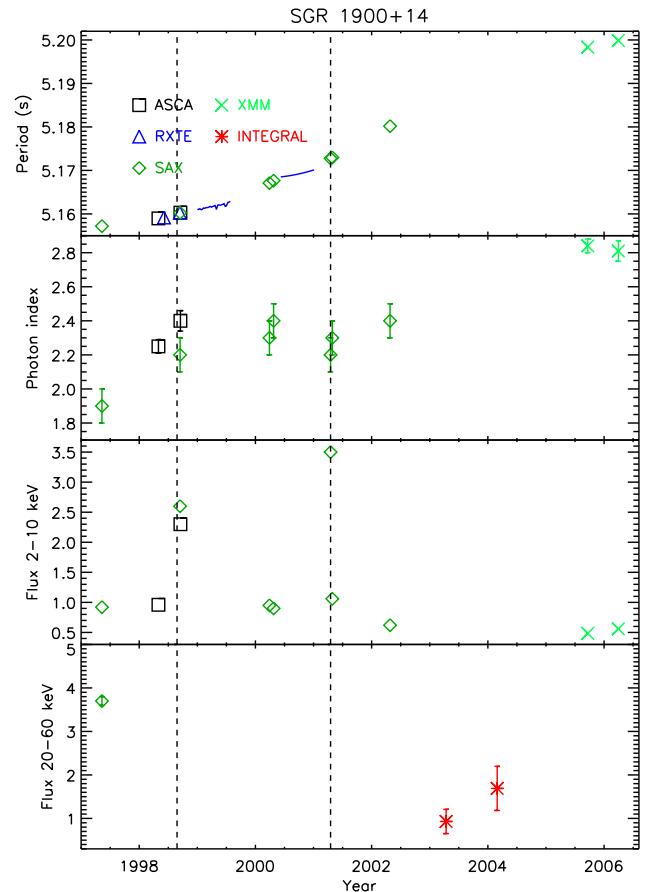


Fig. 7 From top to bottom: long term evolution of the pulse period, photon index, X-ray flux (2–10 keV), and hard X-ray flux (20–60 keV) of SGR 1900+14. Fluxes are in units of 10^{-11} erg cm^{-2} s^{-1} . The vertical dashed lines indicate the 27 August 1998 giant flare and the 18 April 2001 intermediate flare.

value of the magnetic field, repeated scatterings could lead to the formation of a hard tail instead of a narrow line. A different explanation involves vacuum polarization effects. It has been calculated that in strongly magnetized atmospheres this effect can significantly reduce the equivalent width of cyclotron lines, thus making difficult their detection (Ho & Lai 2003).

7 Conclusions

Many of the results presented above fit reasonably well with the magnetar model interpretation. However, there are also a few aspects that require more theoretical and observational efforts to be interpreted in this framework, in particular when one considers the variety of different behaviors shown by these sources and their close relatives like the Anomalous X-ray pulsars (Kaspi 2006).

The long term variations seen in SGR 1806–20, the source observed more often with XMM–Newton, are qualitatively consistent with the predictions of the magnetar model

involving a twisted magnetosphere (Thompson et al. 2002). As mentioned above, according to this model, resonant scattering from magnetospheric currents leads to the formation of a high-energy tail. A gradually increasing twist results in a larger optical depth that causes a hardening of the X-ray spectrum. At the same time, the spin down rate increases because, for a fixed dipole field, the fraction of field lines that open out across the speed of light cylinder grows. In addition, the stresses building up in the neutron star crust and the magnetic footprints movements lead to crustal fractures causing an increase in the bursting activity. Since spectral hardening, spin-down rate, and bursting rate increase with the twist angle, it is not surprising that these quantities varied in a correlated way in SGR 1806–20 (see Fig. 6 and Götz et al. 2006a). However, as visible in Fig. 6, while the spectral hardening took place gradually over several years, the spin-down variation occurred more rapidly in 2000. A recent analysis of RossiXTE data around the time of the giant flare (Woods et al. 2006) shows that the correlation between spectral and variability parameters is indeed rather complex.

The long term flux evolution of SGR 1900+14 is shown in Fig. 7. It can be seen that, excluding the enhancements seen in correspondence of the flares, the luminosity remained always at the same level in the years 1997–2001, and then decreased slightly until the lowest value seen with XMM–Newton in September 2005. The following observation of April 2006 showed that the decreasing luminosity trend has been interrupted by the recent onset of bursts emission. However, the moderate flux increase was not associated with significant changes in the X-ray spectral and timing properties, probably because the source is, up to now, only moderately active.

The luminosity now reached by SGR 1627–41, $\sim 3.5 \times 10^{33}$ erg s⁻¹ is the smallest ever observed from a SGR, and is similar to that of the low state of the transient anomalous X-ray pulsar XTE J1810–197 (Ibrahim et al. 2004; Gotthelf et al. 2004). This low luminosity might be related to the long period (~ 6 years) during which SGR 1627–41 has not emitted bursts. However, the behavior of this source differs from that of the other SGRs that during periods of apparent lack of bursts changed only moderately their luminosity. In fact no bursts were detected from SGR 1900+14 in the three years preceding the XMM–Newton observations: had its luminosity decreased with the same trend exhibited by SGR 1627–41 it would have been much fainter than observed by XMM–Newton. Even more striking is the case of SGR 0526–66, which has a high luminosity ($\sim 2 \times 10^{35}$ erg s⁻¹), despite no signs of bursting activity have been observed in the last 15 years (unless weak bursts from this source have passed undetected due to its larger distance and location in a poorly monitored sky region).

It thus seems that, similarly to the case of Anomalous X-ray Pulsars, SGRs comprise both “persistent” sources (SGR 1806–20, SGR 1900+14 and SGR 0526–66) and “transients” (SGR 1627–41). The reasons behind this difference are currently unclear and not necessarily the same that differentiate between SGRs and AXPs.

Acknowledgements This work has been supported by the Italian Space Agency through the contract ASI-INAF I/023/05/0. XMM–Newton is an ESA science mission with instruments and contributions directly funded by ESA Member States and NASA.

References

- Borkowski J., Götz D., Mereghetti S. et al. GRB Circular Network, **2920** (2004)
- Cameron P.B., Chandra P., Ray A. et al. *Nature*, **434**, 1112 (2005)
- Campbell P., Hill M., Howe R. et al. GRB Circular Network, **2932** (2005)
- Corbel S., Chapuis C., Dame T.M. et al. *ApJ*, **526**, L29 (1999)
- Corbel S. & Eikenberry S.S. *A&A*, **419**, 191 (2004)
- Duncan R.C. & Thompson C. *ApJ*, **392**, L9 (1992)
- Esposito P., Mereghetti S., Tiengo A. et al. Submitted to *A&A* (2006)
- Fenimore E.E., Laros J.G. & Ulmer A. *ApJ*, **432**, 742 (1994)
- Feroci M., Frontera F., Costa E. et al. *ApJ*, **515**, L9 (1999)
- Feroci M., in’t Zand J.J.M., Soffitta P. et al. GRB Circular Network, **1060** (2001)
- Feroci M., Mereghetti S., Woods P. et al. *ApJ*, **596**, 470 (2003)
- Feroci M., Caliendo G.A., Massaro E. et al. *ApJ*, **612**, 408 (2004)
- Figer D.F., Najarro F., Geballe T.R. et al. *ApJ*, **622**, L49 (2005)
- Frail D.A., Vasisht G. & Kulkarni S.R. *ApJ*, **480**, L129 (1997)
- Frail D.A., Kulkarni S.R. & Bloom J.S. *Nature*, **398**, 127 (1999)
- Golenetskii S., Aptekar R., Mazets E. et al. GRB Circular Network, **4936** (2006)
- Gotthelf E.V., Halpern J.P., Buxton M. et al. *ApJ*, **605**, 368 (2004)
- Götz D., Mereghetti S., Mirabel I.F. et al. *A&A*, **417**, L45 (2004)
- Götz D., Mereghetti S. & Hurley K. these proceedings (2006a)
- Götz D., Mereghetti S., Tiengo A. et al. *A&A*, **449**, L31 (2006b)
- Göğüş E., Kouveliotou C., Woods P.M. et al. *ApJ*, **558**, 228 (2001)
- Göğüş E., Kouveliotou C., Woods P.M. et al. *ApJ*, **577**, 929 (2002)
- Guidorzi C., Frontera F., Montanari E. et al. *A&A*, **416**, 297 (2004)
- Ho W.C.G. & Lai D. *MNRAS*, **327**, 1081 (2001)
- Ho W.C.G. & Lai D. *MNRAS*, **338**, 233 (2003)
- Hurley K., Cline T., Mazets E. et al. *Nature*, **397**, 41 (1999a)
- Hurley K., Kouveliotou C., Cline T. et al. *ApJ*, **523**, L37 (1999b)
- Hurley K., Kouveliotou C., Woods P. et al. *ApJ*, **519**, L143 (1999c)
- Hurley K., Li P., Kouveliotou C. et al. *ApJ*, **510**, L111 (1999d)
- Hurley K., Mazets E., Golenetskii S. et al. GRB Coordinates Network, **715** (2002)
- Hurley K., Boggs S.E., Smith D.M. et al. *Nature*, **434**, 1098 (2005)
- Ibrahim A.I., Swank J.H. & Parke W. *ApJ*, **584**, L17 (2003)
- Ibrahim A.I., Markwardt C.B., Swank J.H. et al. *ApJ*, **609**, L21 (2004)
- Israel G.L., Covino S., Mereghetti S. et al. *The Astronomer’s Telegram*, **378** (2005)
- Israel G.L. these proceedings (2006)
- Kaplan D.L., Kulkarni S.R., van Kerkwijk M.H. et al. *ApJ*, **556**, 399 (2001)
- Kaplan D.L., Fox D.W., Kulkarni S.R. et al. *ApJ*, **564**, 935 (2002)
- Kaspi V. these proceedings (2006)
- Kouveliotou C., Fishman G.J., Meegan C.A. et al. *Nature*, **362**, 728 (1993)
- Kouveliotou C., Dieters S., Strohmayer T. et al. *Nature*, **393**, 235 (1998)
- Kouveliotou C., Strohmayer T., Hurley K. et al. *ApJ*, **510**, L115 (1999)
- Kouveliotou C., Tennant A., Woods P.M. et al. *ApJ*, **558**, L47 (2001)
- Kouveliotou C., Eichler D., Woods P.M. et al. *ApJ*, **596**, L79 (2003)
- Kulkarni S.R., Kaplan D.L., Marshall H.L. et al. *ApJ*, **585**, 948 (2003)
- Laros J.G., Fenimore E.E., Fikani M.M. et al. *Nature*, **322**, 152 (1986)
- Marsden D. & White N.E. *ApJ*, **551**, L155 (2001)
- Mazets E.P., Golenetskii S.V. & Guryan Y.A. *Soviet Astronomy Letters*, **5**, 343 (1979)
- Mazets E.P., Aptekar R.L., Butterworth P.S. et al. *ApJ*, **519**, L151 (1999)
- Mazets E.P., Cline T.L., Aptekar R.L. et al. *ArXiv Astrophysics e-prints [ArXiv: astro-ph/0502541]* (2005)

- McClure-Griffiths N.M. & Gaensler B.M. *ApJ*, **630**, L161 (2005)
- Mereghetti S., Cremonesi D., Feroci M. et al. *A&A*, **361**, 240 (2000)
- Mereghetti S., Feroci M., Tavani M. et al. *Memorie della Societa Astronomica Italiana*, **73**, 572 (2002)
- Mereghetti S., Götz D., von Kienlin A. et al. *ApJ*, **624**, L105 (2005a)
- Mereghetti S., Götz D., Mirabel I.F. et al. *A&A*, **433**, L9 (2005b)
- Mereghetti S., Tiengo A., Esposito P., et al. *ApJ*, **628**, 938 (2005c)
- Mereghetti S., Esposito P., Tiengo A. et al. *A&A*, **450**, 759 (2006a)
- Mereghetti S., Esposito P., Tiengo A. et al. Submitted to *ApJ* (2006b)
- Molkov S., Hurley K., Sunyaev R. et al. *A&A*, **433**, L13 (2005)
- Murakami T., Tanaka Y., Kulkarni S.R. et al. *Nature*, **368**, 127 (1994)
- Olive J.-F., Hurley K., Sakamoto T. et al. *ApJ*, **616**, 1148 (2004)
- Palmer D., Barthelmy S., Barbier L. et al. *GRB Circular Network*, **2945** (2005)
- Palmer D., Sakamoto T., Barthelmy S. et al. *The Astronomer's Telegram*, **789** (2006)
- Rea N., Israel G., Covino S. et al. *The Astronomer's Telegram*, **645** (2005)
- Stella L. these proceedings (2006)
- Strohmayr T.E. & Ibrahim A.I. *ApJ*, **537**, L111 (2000)
- Strüder L., Briel U., Dennerl K. et al. *A&A*, **365**, L18 (2001)
- Thompson C. & Duncan R.C. *MNRAS*, **275**, 255 (1995)
- Thompson C., Lyutikov M. & Kulkarni S.R. *ApJ*, **574**, 332 (2002)
- Tiengo A., Esposito P., Mereghetti S. et al. *A&A*, **440**, L63 (2005)
- Turner M.J.L., Abbey A., Arnaud M. et al. *A&A*, **365**, L27 (2001)
- van Kerkwijk M.H., Kulkarni S.R., Matthews K. et al. *ApJ*, **444**, L33 (1995)
- Vasisht G., Kulkarni S.R., Frail D.A. et al. *ApJ*, **431**, L35 (1994)
- Vrba F.J., Henden A.A., Luginbuhl C.B. et al. *ApJ*, **533**, L17 (2000)
- Wachter S., Patel S.K., Kouveliotou C. et al. *ApJ*, **615**, 887 (2004)
- Woods P.M., Kouveliotou C., van Paradijs J. et al. *ApJ*, **524**, L55 (1999a)
- Woods P.M., Kouveliotou C., van Paradijs J. et al. *ApJ*, **518**, L103 (1999b)
- Woods P.M., Kouveliotou C., van Paradijs J. et al. *ApJ*, **519**, L139 (1999c)
- Woods P.M., Kouveliotou C., Finger M.H. et al. *ApJ*, **535**, L55 (2000)
- Woods P.M., Kouveliotou C., Göğüş E. et al. *ApJ*, **576**, 381 (2002)
- Woods P.M. & Thompson C. in "Compact Stellar X-ray Sources", ed. W.H.G. Lewin and M. van der Klis [ArXiv: astro-ph/0406133] (2004)
- Woods P.M., Kouveliotou C., Finger M.H. et al. Submitted to *ApJ* [ArXiv: astro-ph/0602402] (2006)
- Zane S., Turolla R., Stella L. et al. *ApJ*, **560**, 384 (2001)